

Digital holographic tomography based on spectral interferometry

Lingfeng Yu^{1,*} and Zhongping Chen¹

¹Department of Biomedical Engineering, Beckman Laser Institute, University of California, Irvine, Irvine, California 92612, USA

*Corresponding author: yulingfeng@gmail.com

Received June 6, 2007; revised August 28, 2007; accepted September 2, 2007;
posted September 6, 2007 (Doc. ID 83863); published xx xx, xxxx

A digital holographic tomography system has been developed with the use of an inexpensive broadband light source and a fiber-based spectral interferometer. Multiple synthesized holograms (or object wave fields) of different wavelengths are obtained by transversely scanning a probe beam. The acquisition speed is improved compared with conventional wavelength-scanning digital holographic systems. The optical field of a volume around the object location is calculated by numerical diffraction from each synthesized hologram, and all such field volumes are numerically superposed to create the three-dimensional tomographic image.

Experiments were performed to demonstrate the idea. © 2007 Optical Society of America

OCIS codes: 090.1760, 110.6960, 110.0180, 110.6880.

Three-dimensional (3D) digital holographic microscopy has become a subject of increasing interest for many researchers. Although all the 3D information of an object can be recorded by use of a camera, and the object wave field can be reconstructed by numerical algorithms at different positions, the reconstructed image from a single hologram does not automatically provide the 3D tomographic structure of the sample. Both the in-focus layer and the out-of-focus blurs of a thick specimen contribute to a single reconstruction. To resolve the 3D tomographic information in digital holographic microscopy, the specimen needs to be scanned by changing the k vector of the illumination waves according to the well-known optical diffraction tomography theory [1]. This can be accomplished by either changing the relative orientation of the recording wave or, more practically, rotating a transparent or semitransparent specimen with a fixed illumination beam [2], using a broadband source [3] or scanning the wavelength of the illumination beam as in wavelength-scanning digital holographic microscopy (WSDHM) [4–7].

In WSDHM, a set of holograms with a series of wavenumbers was recorded, and the numerical interference of the multiple 3D hologram fields resulted in a synthesized short coherence length and corresponding narrow axial resolution. The axial resolution of WSDHM was determined by the bandwidth of the scanning source, and the nonoverlapping reconstruction extent was determined by the scanning step of the wavenumbers. In all the previously reported WSDHM systems [4–7], one or several expensive frequency-tunable lasers were used for wavelength scanning with a tuning rate of a few nanometers per second. It normally took several minutes to scan hundreds of holograms at this scanning rate. Although high-speed swept sources have been reported, their relative low power limits them for high-speed, full-field applications.

In this Letter, we propose a novel digital holographic tomography (DHT) system based on a fiber-based spectral interferometer. Instead of using tunable lasers, a relatively inexpensive broadband

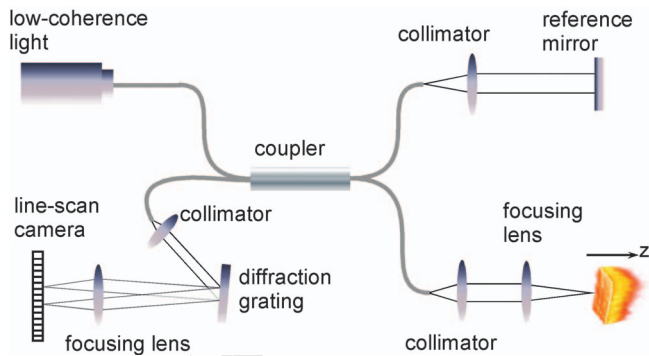
source was used as the light source. Hundreds of 2D “synthesized holograms” (or object wave fields) were obtained by the transversal scanning of a probe beam within a few seconds. Holographic images of an object volume were numerically reconstructed from each synthesized hologram, and tomographic images were obtained by the superposition of all the image volumes. Unlike scanning holography [8], where a holographic record of electronic form was produced by scanning a temporally modulated Fresnel zone pattern over the object, this Letter reports what is believed to be the first time that multiple holograms of different wavelengths were obtained by transversely scanning a probe beam, which could be considered as a successful extension to the current technique of digital holography.

Let us consider the propagation of object fields from multiwavelength recorded holographic fields. If we use \mathbf{r}_p to represent a single point (x_p, y_p, z_p) on the object that scatters the incident beam into a Huygens wavelet $A(\mathbf{r}_p)$, and the above process is repeated with different wavenumbers and all the reconstructed fields are superposed together to give a field [4,7]:

$$E(\mathbf{r}) \sim \int A(\mathbf{r}_p) \int_k S(k) \exp(ik|\mathbf{r} - \mathbf{r}_p|) dk \cdot d^3\mathbf{r}_p \sim \int A(\mathbf{r}_p) M(|\mathbf{r} - \mathbf{r}_p|) d^3\mathbf{r}_p \sim A(\mathbf{r}), \quad (1)$$

where k is the wavenumber, M is the Fourier transform (FT) of the spectral density $S(k)$ and it actually defines the axial resolution of the system. As the number of wavelengths goes to infinite, M actually becomes a delta function; thus, except for a diffraction factor, the resultant field is proportional to the field at the object and is nonzero only at the object points.

The design of the spectral-interferometer-based DHT system is illustrated in Fig. 1. A fiber-based Michelson interferometer is illuminated by a superluminescent diode with a spectrum centered at 1315 nm and a total delivered power of 8 mW. Ap-



Color: Print

Fig. 1. Apparatus for digital holographic tomography system based on spectral interferometry.

ers to find the focus. Here, we propose a new (chromatic) tomographic method to combine the principle of WSDHM with spectral interferometry. High-resolution details can be recovered from outside of the depth-of-focus region with little loss of lateral resolution.

According to Eq. (2), the nonoverlapping positive image can be extracted by properly adjusting the relative position of the reference mirror, and its corresponding spectral information can be Fourier transformed back to k space as

$$I'(k) = S(k)R \int_{-\infty}^{\infty} O(\Delta z) \exp[ik\Delta z + \varphi(\Delta z)] d\Delta z. \quad (3)$$

Note that $I'(k)$ is the spectral information of a single line (A line) along the z axis when the probe beam is illuminating a specific (x, y) position on the sample. Because phase fluctuations exist during 2D scanning of the system, a microscope cover glass (or other surface) is intentionally used as a reference to eliminate the phase fluctuation of different transversal scans. For each A-line scanning, the phase of the reference pixel in the corresponding A-line (z -axis) profile, which represents the front surface of the coverslip, is calculated and subtracted along all pixels of the A line, then the spectral information $I'(k)$ of each A line in Eq. (3) is calculated by taking the FT of the filtered and phase-corrected positive complex image. Thus, by 2D scanning of the galvo system, object wave fields $I'(x, y, k_n)$ with $(n=1, 2, \dots, 1024)$ different wavenumbers are readily available. We noticed that the information $I'(x, y, k)$ at a designated k was equivalent to the extracted object wave field from a 2D hologram recorded with a wavenumber k . According to the principle of WSDHM, a holographic 3D object volume was numerically reconstructed from each $I'(x, y, k)$ by use of a diffraction algorithm, and all the 3D arrays are numerically superposed together, resulting in an accumulated field distribution that represents the 3D object structure.

Experiments were performed to prove the effectiveness of the proposed method. The diameter of the probe beam was 4.8 mm and an objective of 40 mm focal length was used, which resulted in a $\sim 13.8 \mu\text{m}$ lateral resolution and $\sim 230 \mu\text{m}$ DOF in vacuum. A U.S. Air Force (USAF) 1951 resolution target was placed 1.8 mm away from the DOF region of the probe beam with a clear pattern on a flat chrome background facing to the right in Fig. 1. The galvo system scanned an area of $1.5 \text{ mm} \times 1.5 \text{ mm}$ with 300×300 pixels. Here the uncoated target surface was used as the reference for phase correction. Figures 2(a) and 2(b) show the amplitude and phase information of the target before phase correction for k_{512} , respectively. Phase fluctuations are evident in Fig. 2(b). Since the target was not well focused, the diffraction effect of the pattern is clearly seen in Fig. 2(a). Figure 2(c) shows the phase map of the reference plane (uncoated target surface) and Fig. 2(d) shows the corrected phase map of the target. The angular spectrum method [4] was then used to numerically find the focus of the object as in Fig. 2(e). For

approximately half of the power goes to the sample arm. The full width at half maximum (FWHM) of the source is $\sim 95 \text{ nm}$, and its coherence length is $\sim 8 \mu\text{m}$. Backreflected lights from the reference and sample arms are guided into a spectrometer and sampled by a 1×1024 line-scan camera (SU1024-1.7T, Sensors Unlimited) at 7.7 kHz. The captured spectrogram in the camera is linearly interpolated as 1024 evenly k -spaced wavelengths extending from 1250.623 to 1373.190 nm, corresponding to a spectral resolution of 0.12 nm and an imaging depth of 3.6 mm in vacuum. The interference between the two arms is recorded in the frequency domain as [9,10]:

$$I(k) = S(k)R^2 + S(k) \int_{-\infty}^{\infty} \int_{-\infty}^{\infty} O(\Delta z)O(\Delta z') \times \exp[ik(\Delta z - \Delta z') + \varphi(\Delta z) - \varphi(\Delta z')] d\Delta z d\Delta z' + 2S(k)R \int_{-\infty}^{\infty} O(\Delta z) \cos(k\Delta z + \varphi(\Delta z)) d\Delta z, \quad (2)$$

where R and O represent the amplitude of the reference and object signals, respectively. Δz and $\Delta z'$ denote the double-pass path-length difference between the sample and the reference mirror, and φ is the phase term of object signals. The first two terms yield dc and low-frequency noises, and the last term contains the depth information of the object and can be obtained by an inverse FT from k to z space. Note that the inverse FT of the last term gives symmetric positive and negative images in space. The system is similar to Fourier domain optical coherence tomography (FDOCT) [9–12], a powerful imaging technique that has attracted a great deal of attention recently. The axial resolution of the proposed arrangement is determined by the coherence length of the light source, and high axial resolution can be achieved independently of the beam-focusing conditions. The lateral resolution is determined by the diameter d of a probe beam and the focal length f of the objective as [12] $\Delta x = 4\lambda f / (\pi d)$. However, only a very small range around the depth-of-field (DOF) exhibits the desired lateral resolution; the probe beam outside the DOF will be largely expanded and the obtained image will be blurred. The monochromatic numerical diffraction method [13] was previously reported to simulate the wave-propagation process from out-of-focus scatter-

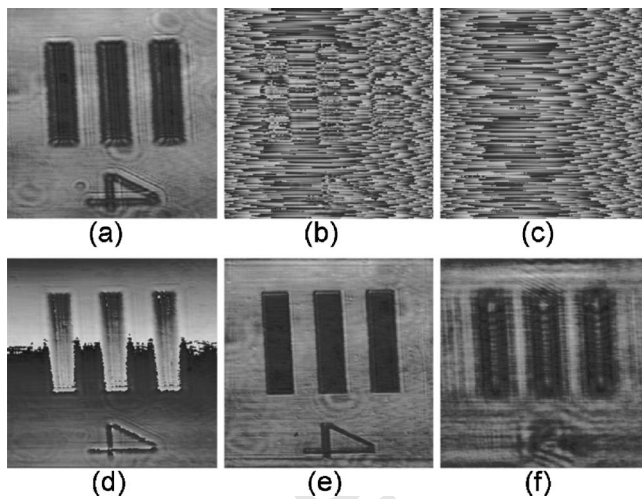


Fig. 2. (a) Amplitude and (b) phase maps of the target without phase correction for a single wavenumber k_{512} , (c) phase map of the reference plane, (d) corrected phase map of the target, (e) reconstructed amplitude image with $z = 1.8$ mm and (f) $z = 10$ mm.

201 comparison, Fig. 2(f) also shows a blurred result
202 when the reconstruction distance is not correctly chosen.
203 The above clearly demonstrates the idea of a
204 “synthesized hologram.” Each synthesized hologram
205 is equivalent to one recorded in conventional digital
206 holography and can be used for numerical reconstruction
207 by diffraction algorithms.

208 Figure 3 shows another example of an ~ 400 μm
209 thick onion slice placed ~ 100 μm away from the
210 DOF region of the probe beam. The use of an objective
211 ($20\times$, Nacet) in this example improved the lateral
212 resolution to ~ 3.5 μm but decreased the DOF to

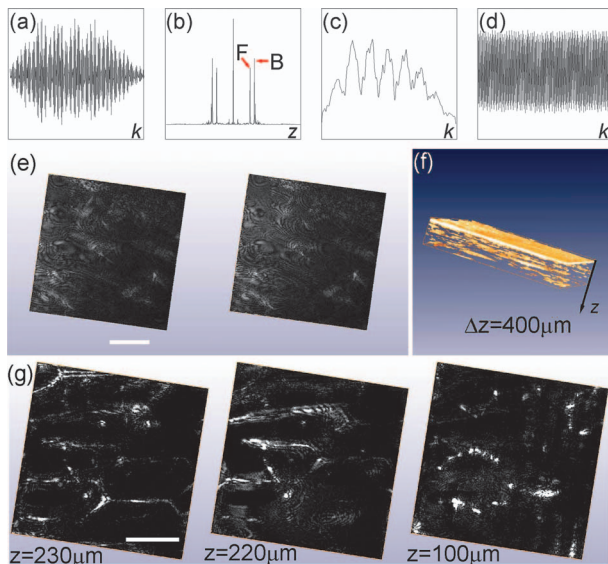


Fig. 3. (a) Spectral interferogram and (b) its inverse FT for one A-line scanning; the phase-corrected positive image is Fourier transformed to get the (c) amplitude and (d) phase of a complex spectral counterpart $I'(k)$ of the positive image, (e) absolute object wave fields $I'(x, y, k)$ for k_{256} and k_{512} , respectively, (f) 3D reconstruction of the onion slice, (g) tomographic images of different depths. The vertical scales in (a)–(d) are normalized and the scale bar represents 100 μm .

14.4 μm . Figure 3(a) shows the spectral interferogram $I(k)$ of one A-line scan and Fig. 3(b) shows its inverse FT. The peak “F” in the figure represents the front surface of an added microscope cover glass and peak “B” shows its back surface. The phase of the peak F was used as the reference for all pixels of the A line. Then, the phase-corrected positive image was filtered and Fourier transformed back to obtain a complex $I'(k)$, whose amplitude and phase information are plotted in Figs. 3(c) and 3(d), respectively. After 2D scanning, the total acquisition time of 1024 synthesized holograms takes ~ 10 s, which could be further improved by using a line-scan camera of higher speed. Figure 3(e) shows two of these holograms. Based on all (or part of) these holograms, the algorithm of WSDHM is then utilized to reconstruct the tomographic images of the sample. Figure 3(f) shows a 3D reconstruction of the sample, and Fig. 3(g) shows several reconstructed tomographic images located at different depths. Note that artifacts may exist in the tomographic reconstruction if the phase information is not correctly obtained because of multiple factors, such as the phase instability of the system or existence of multiple scatterings, etc.

In conclusion, we have demonstrated that multiple k -related 2D synthesized holograms can be obtained by transversely scanning a probe beam in a fiber-based spectral interferometric system. A broadband light source was used as a substitute for relatively expensive tunable lasers for wavelength scanning. The principle of WSDHM was then applied for tomographic reconstruction based on these synthesized holograms. In addition, the acquisition rate of the proposed system was improved compared with conventional WSDHM systems [4–7].

This work was supported by research grants from the National Institutes of Health (EB-00293, NCI-91717, and RR-01192), Air Force Office of Scientific Research (FA9550-04-1-0101), and the Beckman Laser Institute Endowment.

References

1. A. F. Fercher, H. Bartelt, H. Becker, and E. Wiltchko, *Appl. Opt.* **18**, 2427 (1979).
2. F. Charrière, A. Marian, F. Montfort, J. Kuehn, T. Colomb, E. Cuhe, P. Marquet, and C. Depeursinge, *Opt. Lett.* **31**, 178 (2006).
3. L. Martínez-León, G. Pedrini, and W. Osten, *Appl. Opt.* **44**, 3977 (2005).
4. L. Yu and M. K. Kim, *Opt. Lett.* **30**, 2092 (2005).
5. F. Montfort, T. Colomb, F. Charrière, J. Kühn, P. Marquet, E. Cuhe, S. Herminjard, and C. Depeursinge, *Appl. Opt.* **45**, 8209 (2006).
6. L. Yu and M. K. Kim, *Opt. Express* **13**, 5621 (2005).
7. L. Yu and Z. Chen, *Opt. Express* **15**, 878 (2007).
8. T.-C. Poon, K. Doh, B. Schilling, M. Wu, K. Shinoda, and Y. Suzuki, *Opt. Eng. (Bellingham)* **34**, 1338 (1995).
9. F. Fercher, C. K. Hitzenberger, G. Kamp, and S. Y. Elzaiat, *Opt. Commun.* **117**, 43 (1995).
10. G. Häusler and M. W. Lindner, *J. Biomed. Opt.* **3**, 21 (1998).
11. M. Wojtkowski, V. J. Srinivasan, T. H. Ko, J. G. Fujimoto, A. Kowalczyk, and J. S. Duker, *Opt. Express* **12**, 2404 (2004).

- ²⁷⁶ 12. B. E. Bouma and G. J. Tearney, *Handbook of Optical* ²⁷⁸
²⁷⁷ *Coherence Tomography* (Dekker, 2002). Chen, *Opt. Express* **15**, 7634 (2007). ²⁷⁹

PROOF COPY [83863] 512720OPL